

# Asymmetric Faraday Effect in a Magnetophotonic Crystal

D.O. Ignatyeva,<sup>1,2,3,\*</sup> T.V. Mikhailova,<sup>3</sup> P.O. Kapralov,<sup>2</sup> S.D. Lyashko,<sup>3</sup> V.N. Berzhansky,<sup>3</sup> and V.I. Belotelov<sup>3,1,2</sup>

<sup>1</sup>*Photonic and Quantum technologies school, Faculty of Physics,  
Lomonosov Moscow State University, Leninskie gori, 119991 Moscow, Russia*

<sup>2</sup>*Russian Quantum Center, 121205 Moscow, Russia*

<sup>3</sup>*Institute of Physics and Technology, V.I. Vernadsky Crimean Federal University, 295007 Simferopol, Crimea*

(Dated: September 12, 2023)

It is widely known that the magneto-optical Faraday effect is linear in magnetization and therefore the Faraday angles for the states with opposite magnetizations are of opposite sign but equal in modulus. Here we experimentally study propagation of light through a one-dimensional all-garnet magnetophotonic crystal to demonstrate an asymmetric Faraday effect (AFE) for which Faraday angles for opposite magnetic states differ not only in sign but in the absolute value as well. AFE appears in the vicinity of the cavity resonance for an oblique incidence of light which plane of polarization is inclined to the incidence plane. Under proper incidence and polarization angles the magnitude of AFE could be very large reaching 30% of the absolute value of the Faraday effect. The effect originates from the difference in Q-factors for p- and s- polarized cavity modes that breaks the symmetry between the two opposite directions of polarization rotation. The discovered AFE is of prime importance for nanoscale magnonics and optomagnetism.

The first phenomenon which demonstrated interaction between magnetism and optics and established a basis for modern magnetophotonics is the Faraday effect - transformation of polarization of light passing through a magnetized material. It was discovered by Michael Faraday in 1846 [1]. The Faraday effect is characterized by the Faraday rotation angle of the polarization plane of light transmitted through a material along its magnetization. The internal mechanism of the effect is in magnetic circular birefringence, i.e. the magnetization-induced difference in the phase velocities of two circular polarizations with opposite helicities [2]. The Faraday effect is known to be odd in magnetization and thus has a nonreciprocal character [3–6]. Initially, the Faraday’s discovery had a purely fundamental significance, but a lot of applications of the magneto-optics for data storage, fiber-optic communication lines (isolators, modulators, deflectors) [7–9], sensors [10–12] and magnetometry [13, 14] have been suggested in the following decades [15]. For further progress in this direction, it is necessary to find some ways for enhancement and advanced control of the Faraday effect.

Fabrication of nanostructures is the most common solution that has been widely used over some decades to increase the magneto-optical (MO) effects. It is possible to design a system which exhibits an enhanced MO response by concentrating the electromagnetic field of light inside magneto-optically active components in the magnetophotonic crystals (MPCs) with localized states [16–22], guided modes [23–26], in magnetoplasmonic structures [14, 27–33] and metasurfaces [34–38]. Enhancement of the Faraday rotation most often occurs due to an increase in purely magneto-optical contribution (multi-pass mode and localization of light). Additionally, such structures may include the pure optical effects of anisotropy or

reducing the reflectivity to enhance the conversion of polarization state (magnetoplasmonic structures [39–41] or multilayer structures at oblique incidence [42, 43]). The combination of pure magneto-optical and optical mechanisms is responsible for various types of the Faraday effect enhancement [19, 31, 43–47].

Oblique incidence of light onto magnetic films and structures brings some peculiarities of the MO effects [48] which are related to a lower reflectance of p-polarized light with respect to s-polarization. Thus, the odd MO intensity effect appears in the Faraday configuration [49]. In MPCs, the Fresnel coefficients at oblique incidence set different interference conditions for s- and p-polarized light. Thus the same MPC has a higher optical Q-factor for s-polarized light and lower Q-factor for p-polarized light [43, 45–47, 50]. An s-polarized wave demonstrates a higher localization of electromagnetic field inside the MO active cavity and layers, and, therefore, higher values of the Faraday rotation [43]. Furthermore, for MPC with negligible absorption, a wave converted into s-polarized state due to the Faraday effect can be trapped inside the MO active cavity at the Brewster’s angle [46].

In all of the aforementioned studies, the Faraday rotation was odd in magnetization, i.e., reversing the direction of the external magnetic field changed its sign but not its magnitude (see Supplementary S1). In this work, we discover that an additional spatial symmetry break might lead to an even magnetization contribution to the magneto-optical Faraday rotation and, therefore, the emergence of the asymmetric Faraday effect (AFE), which changes not only its sign but also its value if the magnetic field is reversed. We observe such peculiar Faraday effect by illuminating a microcavity MPC with obliquely incident light of some intermediate polarization between pure s- and p-ones. Breaking the oddness of the Faraday effect provides a unique possibility to observe magneto-optical polarization rotation even in the material with non-uniform magnetization direction and zero

\* ignatyeva@physics.msu.ru

net magnetization.

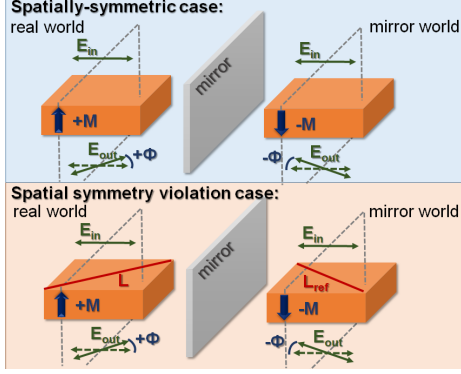


FIG. 1. Schematic representation of spatial symmetry origin of the oddness of the Faraday effect and its violation in the case of symmetry breaking by a director  $L$ .

Let's discuss how the spatial symmetry causes the oddness of the Faraday rotation in the usual case and how it is modified if the spatial symmetry is broken. Figure 1 illustrates the discussed phenomenon from the point of view of what an observer might see in the real world and looking into a mirror. The mirror is placed in the plane of the magnetization  $\mathbf{M}$ , see Fig. 1. One might see in the mirror an oppositely magnetized medium with  $-\mathbf{M}$ , as  $\mathbf{M}$  is an axial vector. At the same time, the director (a director is a quasi-vector with the two equivalent opposite directions)  $\mathbf{E}$  describing the light polarization is transformed by usual reflection rules in the mirror, so that the angle between the reflected  $\mathbf{E}$  and the mirror is opposite to the angle between the real  $\mathbf{E}$  and the mirror. Thus, the magneto-optical polarization rotation caused by passing through a magnetized medium that is observed in the mirror world with  $-\mathbf{M}$  magnetization is equal in magnitude and opposite in sign to the one observed in the real world (Fig. 1):  $-\Phi(\mathbf{M}) = \Phi(-\mathbf{M})$  and, therefore, the magneto-optical rotation is odd in magnetization.

The situation changes if the spatial symmetry of the considered configuration (including both the light and the structure) is broken with respect to the reflection in the mirror placed along  $\mathbf{M}$  due to the presence of the preferred direction described by a director  $L$  (see Fig. 1, bottom panel). Actually, such a preferred direction could arise due to the presence of some vector describing the light or the structure in the considered configuration, too. It might be considered a partial case of the symmetry break described by a director; therefore, in the following we will consider a more general case of a director. Since a director is transformed by usual reflection rules, the configuration in the mirror characterized by the reflected director  $L^{\text{ref}}$  and polarization  $\mathbf{E}$  differs from one observed in the real world, except for the case when  $L$  is perpendicular or parallel to  $\mathbf{E}$ . By repeating the considerations similar to the ones made above, one concludes that  $\Phi(-\mathbf{M}, L^{\text{ref}}) = -\Phi(\mathbf{M}, L)$ , so the absolute

values of  $\Phi$  that are equal to each other refer to different structures:  $|\Phi(\mathbf{M}, L^{\text{ref}})| = |\Phi(\mathbf{M}, L)|$ . At the same time, there are no limitations on the values of  $\Phi$  for the structures with the same  $L$ ;  $|\Phi(-\mathbf{M}, L)|$  and  $|\Phi(\mathbf{M}, L)|$  may differ from each other. Consequently, we can conclude that if  $L$  is oblique with respect to the polarization  $\mathbf{E}$ , then the asymmetric Faraday effect (AFE) is allowed:  $|\Phi(\mathbf{M}, L)| \neq |\Phi(-\mathbf{M}, L)|$ . However, if  $L$  is parallel or perpendicular to  $\mathbf{E}$ , then the AFE is prohibited:  $|\Phi(\mathbf{M})| = |\Phi(-\mathbf{M})|$ .

Such an impact of the spatial symmetry violation described by the director  $L$  might also be understood as the arisen non-equivalence between the clock- and counterclockwise rotation directions. In particular, such non-equivalence reveals itself as the difference between the two opposite directions of the magneto-optical rotations of linear polarization corresponding to the opposite magnetizations (see also Supplementary S4 and Fig. S4.2). Obviously, if  $\mathbf{E}$  is not parallel or perpendicular to  $L$ , then its rotation in counter- and clockwise directions results in different configurations described by a mutual orientation of  $\mathbf{E}$  and  $L$ . Actually, the non-equivalence of counter- and clockwise rotations, as well as the non-equivalence of the 'real-world' and 'mirror-world' configurations, are known as manifestations of the chirality phenomenon. The considerations made above show that such a chiral-type impact on the Faraday effect caused by the presence of the director  $L$  tilted with respect to the polarization  $\mathbf{E}$  describing the structure symmetry could arise in non-chiral nanostructures and films.

It is important that such a symmetry break can be introduced by the design of a nanostructure (for example, by depositing a 1D grating on top of the magnetic film, Supplementary S4) or by incident light itself: an oblique incidence gives birth to the in-plane component of the light wavevector  $k_\tau$ . In this case,  $k_\tau$  determines the direction of  $L$  in the general consideration above. Such a configuration can be implemented in almost any type of magneto-optical structure, including smooth films and crystals (see Supplementary S4). In the present work, we chose this option to introduce a symmetry break by the oblique incidence and demonstrate an asymmetric behavior of the Faraday rotation in MPC.

The MPC consists of two magnetic Bragg mirrors containing pairs of magnetic and nonmagnetic quarter-wave layers and a magnetic half-wave cavity layer sandwiched in between the mirrors (Fig. 2a). It is illuminated by a linearly polarized light incident on the sample at the incidence angle  $\theta$ . Orientation of the light polarization is determined by the angle  $\Psi$  formed by  $\mathbf{E}$  and the plane of light incidence:  $\Psi = 0^\circ$  for the p-polarized light, and  $\Psi = 90^\circ$  for the s-polarized light (Fig. 2a). On the other hand,  $\Psi$  is also an angle between  $k_\tau$  and  $\mathbf{E}$ , and, consequently, it defines the spatial symmetry violation described above. We will focus our attention on the intermediate configuration  $0 < \Psi < 90^\circ$ , for which a spatial symmetry break takes place and AFE is expected.

The asymmetric Faraday effect can be characterized

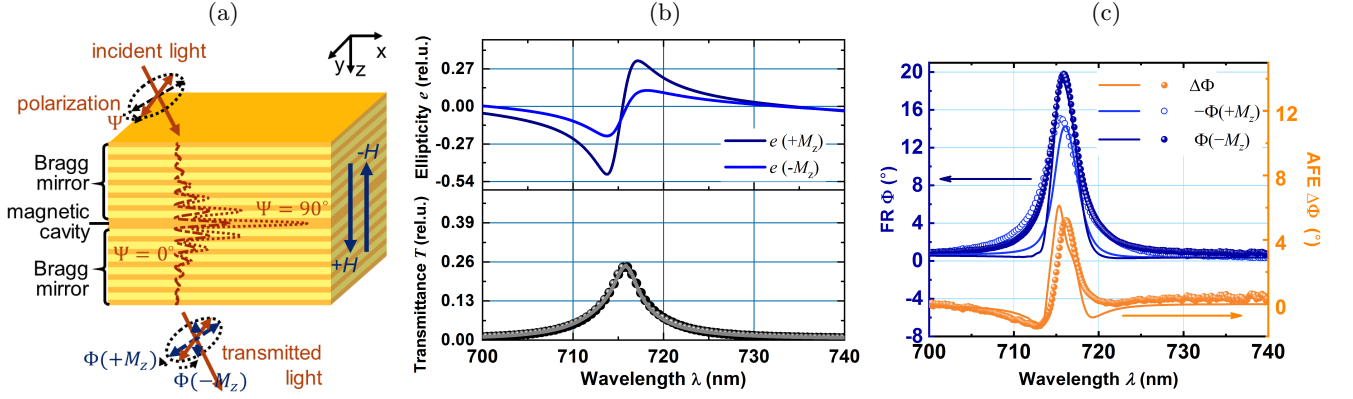


FIG. 2. (a) Schematic diagram of the investigated MPC on the GGG substrate. Optical ellipticity (b, top), transmittance (b, bottom), and the asymmetric Faraday effect (c) spectra of the MPC for the oblique illumination at  $\theta = 63^\circ$ ,  $\Psi = 70^\circ$ . Experimental data is presented by color spheres, while simulations - by solid curves.

by  $\Delta\Phi$ :

$$\Delta\Phi = \Phi(+M_z) - (-\Phi(-M_z)) \quad (1)$$

where  $\Phi(+M_z)$  and  $\Phi(-M_z)$  are the Faraday rotation angles at opposite orientations of the magnetization vector  $\mathbf{M}$  aligned along  $z$  axis. Here we determine the Faraday angles as the difference between the total polarization rotation angles for the sample magnetized  $\pm M_z$  and not magnetized  $M_z = 0$  along  $z$ -axis, therefore, purely optical polarization modification is omitted.

Experimental observation of the asymmetric Faraday effect was performed on the all-garnet MPC (Fig. 2a). The MPC Bragg mirrors consist of six pairs of diamagnetic  $\text{Sm}_3\text{Ga}_5\text{O}_{12}$  (SGG) and the MO active ferromagnetic  $\text{Bi}_{2.97}\text{Er}_{0.03}\text{Al}_{0.5}\text{Ga}_{0.5}\text{O}_{12}$  (BIG) garnet layers ( $h_{\text{BIG}} = 75$  nm,  $h_{\text{SGG}} = 100$  nm) synthesized by RF-magnetron sputtering on (111)  $\text{Gd}_3\text{Ga}_5\text{O}_{12}$  (GGG) substrate [51, 52]. There is a cavity layer of BIG in between the Bragg mirrors:  $\text{GGG} / [\text{BIG} / \text{SGG}]^6 / 2 \text{BIG} / [\text{SGG} / \text{BIG}]^6$  responsible for a cavity mode (see Supplementary S2 and S3 for the details).

The Faraday rotation was experimentally found using a conventional scheme where the transmitted light intensity  $I_{\text{out}}$  is measured in the presence of polarizer and analyzer crossed by angle of  $45^\circ$ , so that  $I_{\text{out}} = \frac{1}{2} I_0 \cdot (1 - \sin(2\text{OR} + 2\Phi))$ , where OR is a purely optical non-magnetic polarization rotation, and  $I_0$  is the intensity of the light transmitted through the MPC without a polarizer (see Supplementary S3.3 for the details). Strictly speaking, this formula is not valid in the presence of ellipticity in the sample. But still it can be applied in the vicinity of the cavity resonance since the ellipticity vanishes at the resonant wavelength (Fig. 2b).

We chose at first the polarization angle  $\Psi = 70^\circ$ . Both experimental measurements (color spheres in Fig. 2b) and numerical simulations performed using the transfer matrix method  $4 \times 4$  [53] (solid curves in Fig. 2b, see Supplementary S2 for simulation details) show that at the oblique incidence the cavity mode is observed at

$\lambda = 716$  nm for  $\theta = 63^\circ$ . The cavity resonance is accompanied with a pronounced peak of the Faraday rotation  $\Phi \sim 20^\circ$  (Fig. 2c), which gives a high magneto-optical quality factor  $Q_{\text{MO}} = -2|\Phi|/\ln T = 42.6^\circ$  and MO figure of merit  $\text{MOFOM} = T \sin 2\Phi = 20\%$  [21].

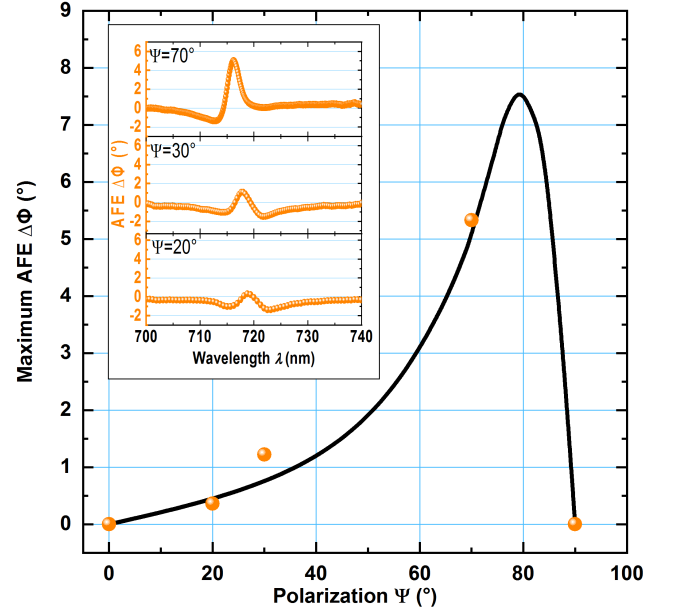


FIG. 3. The dependence of the asymmetric Faraday effect on the initial light polarization  $\Psi$  for  $\theta = 63^\circ$ . The inset shows the AFE spectra for  $\Psi = 20^\circ, 30^\circ, 70^\circ$ . Experimental data is presented by color spheres, while simulations - by solid curve.

At  $\Psi = 70^\circ$  a notable AFE characterized by  $\Delta\Phi = 5.5^\circ$  appears in the vicinity of the cavity resonance (Fig. 2c). Since at this wavelength  $\Phi \sim 20^\circ$ , it means that AFE accounts about 30% of the Faraday effect. Similar AFE is observed for oblique incidence of any intermediate polarization of light and vanishes only for pure p- or s-polarizations for which there is no spatial symmetry violation since in those cases  $k_\tau$  is either parallel or per-

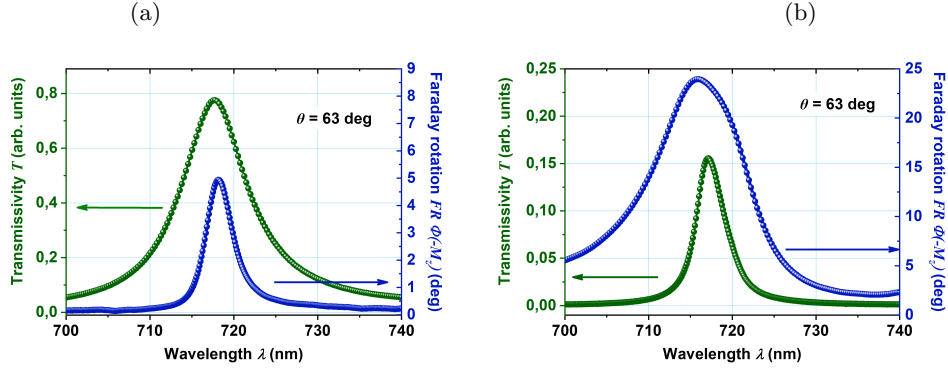


FIG. 4. Spectra of transmittance and Faraday rotation at the oblique incidence of  $\theta = 63$  deg for (a) p- and (b) s-polarized light (experiments).

pendicular to  $\mathbf{E}$ , respectively (Fig. 3). The largest value of AFE appears at  $\Psi = 80^\circ$  and equals to  $\Delta\Phi = 7.5^\circ$ , which is 38% of the  $\Phi$  value.

As we discussed above, in our experiments, the difference between  $|\Phi(+M_z)|$  and  $|\Phi(-M_z)|$  for intermediate  $\Psi$  values appears due to the break of the spatial symmetry defined by  $k_\tau$ . This symmetry break gives birth to the even in magnetization terms of the Faraday rotation:  $\Phi(M_z) = \phi_1 \frac{M_z}{M_{z0}} + \phi_2 \left( \frac{M_z}{M_{z0}} \right)^2 + \dots$  (where  $M_{z0}$  is the saturation magnetization and  $\phi_j$  are the expansion coefficients). In the 'usual' cases of normal incidence, or pure p- or s-polarized light at the oblique incidence, which are used in most of the magneto-optical experiments,  $\phi_2 = \phi_{2n} = 0$ , where  $n$  is an integer (see Supplementary S1.2).

As AFE is a nonlinear part of the Faraday rotation, one might expect to observe high AFE in cases where the linear Faraday effect is large. From this point of view, MPCs at oblique incidence are the ideal candidates to observe AFE. On the one hand, they possess a high Faraday rotation of tens of degrees (see blue lines in Figs. 4a,b). On the other hand, they exhibit a prominent difference between the p- and s- polarized states. The origin of this difference is the variation of the reflectivity of the Bragg mirrors surrounding the cavity layer, leading to a difference in Q-factors. Figure 4 demonstrates a more than 5-fold difference in the transmittance (green lines) and Faraday rotation (blue lines) for p-polarized (Fig. 4a) and s-polarized (Figure 4b) light (see also Supplementary S3.2). Thus, MPC properties are very sensitive to the mutual orientations of  $\mathbf{E}$  and  $\mathbf{k}_\tau$  vectors, which clearly differentiates  $\Psi + \Phi$  and  $\Psi - \Phi$  states corresponding to the opposite rotation directions. This provides large values of AFE. For the considered MPC, the second-order term contribution grows significantly up to  $\phi_2/\phi_1 = 0.19$ . For a comparison, in a smooth film of the same thickness, the quadratic term is very small:  $\phi_2/\phi_1 = 0.009$  (see Supplementary S4). Therefore, the role of the MPC here is to enhance the AFE and make it easily measurable.

The Faraday effect is commonly used for the magneto-optical studies of the magnetic materials and magneti-

zation distributions. However, the obvious difficulties arise if the magnetization distribution is non-uniform so that the net magnetization in the area illuminated by the probe beam is zero:  $\int_{S_{\text{beam}}} M_z(x, y) dx dy = 0$ . This situation takes place, for example, for macroscopic static subwavelength domain structures [54] and dynamic  $M_z$  oscillations in ultrashort spin waves [55, 56] and spin-wave resonances [24]. Although there is magnetization in each spatial point of the material, the Faraday rotation is absent due to the zero average  $\langle M_z \rangle$  in the illuminated area. The situation changes if the spatial symmetry break is used to produce AFE, for example, as demonstrated in the present work. Even if the net magnetization is zero, AFE makes it possible to measure the polarization rotation arisen due to the non-zero  $\langle M_z^2 \rangle$ . This opens a unique possibility to study various types of materials with inhomogeneous static or dynamic spatial magnetization distributions.

Therefore, here we demonstrate the asymmetric Faraday effect that arises if an additional symmetry break with respect to the reflection in a mirror parallel to magnetization is introduced to the magneto-optical system. We confirm this prediction by studying the magneto-photonic crystal at oblique incidence, which provides a unique modification of the Faraday effect's symmetry and magnetization dependence. Experimentally, a pronounced asymmetry of the Faraday rotation spectra for oppositely directed magnetic fields reaching  $|\Phi(+M_z)| - |\Phi(-M_z)| \sim 30\%$  is obtained. Such behavior results from a strong non-equivalence of the counter- and clockwise magneto-optical rotations of linear polarization and brings the quadratic in the magnetization term to the Faraday rotation spectra. For the magnetophotonic crystal, this quadratic term has the same order of magnitude as the linear one, providing a unique possibility to observe magneto-optical polarization rotation even in the material with a non-uniform magnetization direction and zero net magnetization. At the same time, we show that AFE is a quite general effect that might be observed in various structures with a particular type of spatial symmetry breaking. This is a key feature for optical studies

of the static and dynamic magnetic patterns with zero net magnetization and ultrashort spin waves [55, 56].

## ACKNOWLEDGMENTS

This work was financially supported by the Ministry of Science and Higher Education of the Russian Federation,

Megagrant project No. 075-15-2022-1108. The authors thank A.N. Kalish and A.A.Voronov for the fruitful discussion.

- 
- [1] M. Faraday, On the magnetization of light and the illumination of magnetic lines of force, *Philosophical Transactions of the Royal Society of London* **136**, 1 (1846).
  - [2] A. K. Zvezdin and V. A. Kotov, *Modern magnetooptics and magneto-optical materials* (CRC Press, 1997).
  - [3] J.-P. Krumme, V. Doormann, and C.-P. Klages, Measurement of the magneto-optic properties of bismuth-substituted iron garnet films using piezobirefringent modulation, *Applied optics* **23**, 1184 (1984).
  - [4] G. F. Dionne and G. A. Allen, Molecular-orbital analysis of magneto-optical bi-o-fe hybrid excited states, *Journal of Applied Physics* **75**, 6372 (1994).
  - [5] M. Deb, E. Popova, A. Fouchet, and N. Keller, Magneto-optical faraday spectroscopy of completely bismuth-substituted bi3fe5o12 garnet thin films, *Journal of Physics D: Applied Physics* **45**, 455001 (2012).
  - [6] C. Caloz, A. Alu, S. Tretyakov, D. Sounas, K. Achouri, and Z.-L. Deck-Léger, Electromagnetic nonreciprocity, *Physical Review Applied* **10**, 047001 (2018).
  - [7] D. Karki, R. El-Ganainy, and M. Levy, Toward high-performing topological edge-state optical isolators, *Physical Review Applied* **11**, 034045 (2019).
  - [8] K.-S. Ho, S.-J. Im, J.-S. Pae, C.-S. Ri, Y.-H. Han, and J. Herrmann, Switchable plasmonic routers controlled by external magnetic fields by using magneto-plasmonic waveguides, *Scientific reports* **8**, 1 (2018).
  - [9] W. Śmigaj, J. Romero-Vivas, B. Gralak, L. Magdenko, B. Dagens, and M. Vanwolleghem, Magneto-optical circulator designed for operation in a uniform external magnetic field, *Optics letters* **35**, 568 (2010).
  - [10] N. Maccaferri, K. E. Gregorczyk, T. V. De Oliveira, M. Kataja, S. Van Dijken, Z. Pirzadeh, A. Dmitriev, J. Åkerman, M. Knez, and P. Vavassori, Ultrasensitive and label-free molecular-level detection enabled by light phase control in magnetoplasmonic nanoantennas, *Nature communications* **6**, 1 (2015).
  - [11] D. Ignatyeva, P. Kapralov, G. Knyazev, S. Sekatskii, G. Dietler, M. Nur-E-Alam, M. Vasiliev, K. Alameh, and V. Belotelov, High-q surface modes in photonic crystal/iron garnet film heterostructures for sensor applications, *JETP letters* **104**, 679 (2016).
  - [12] O. Borovkova, D. Ignatyeva, S. Sekatskii, A. Karabchevsky, and V. Belotelov, High-q surface electromagnetic wave resonance excitation in magnetophotonic crystals for supersensitive detection of weak light absorption in the near-infrared, *Photonics Research* **8**, 57 (2020).
  - [13] D. O. Ignatyeva, G. A. Knyazev, A. N. Kalish, A. I. Chernov, and V. I. Belotelov, Vector magneto-optical magnetometer based on resonant all-dielectric gratings with highly anisotropic iron garnet films, *Journal of Physics D: Applied Physics* **54**, 295001 (2021).
  - [14] G. A. Knyazev, P. O. Kapralov, N. A. Gusev, A. N. Kalish, P. M. Vetoshko, S. A. Dagesyan, A. N. Shaposhnikov, A. R. Prokopov, V. N. Berzhansky, A. K. Zvezdin, *et al.*, Magnetoplasmonic crystals for highly sensitive magnetometry, *ACS Photonics* **5**, 4951 (2018).
  - [15] M. Inoue, M. Levy, and A. V. Baryshev, *Magnetophotonics: From theory to applications* (Springer Science & Business Media, 2013).
  - [16] M. Inoue, R. Fujikawa, A. Baryshev, A. Khanikaev, P. Lim, H. Uchida, O. Aktsipetrov, A. Fedyanin, T. Murzina, and A. Granovsky, Magnetophotonic crystals, *Journal of Physics D: Applied Physics* **39**, R151 (2006).
  - [17] A. Zhdanov, A. Fedyanin, O. Aktsipetrov, D. Kobayashi, H. Uchida, and M. Inoue, Enhancement of faraday rotation at photonic-band-gap edge in garnet-based magnetophotonic crystals, *Journal of Magnetism and Magnetic Materials* **300**, e253 (2006).
  - [18] I. Lyubchanskii, N. Dadoenkova, M. Lyubchanskii, E. Shapovalov, and T. Rasing, Magnetic photonic crystals, *Journal of Physics D: Applied Physics* **36**, R277 (2003).
  - [19] N. Maccaferri, I. Zubritskaya, I. Razdolski, I.-A. Chioar, V. Belotelov, V. Kapaklis, P. M. Oppeneer, and A. Dmitriev, Nanoscale magnetophotonics, *Journal of Applied Physics* **127**, 080903 (2020).
  - [20] A. Merzlikin, A. Vinogradov, A. Dorofeenko, M. Inoue, M. Levy, and A. Granovsky, Controllable tamm states in magnetophotonic crystal, *Physica B: Condensed Matter* **394**, 277 (2007).
  - [21] T. Mikhailova, V. Berzhansky, A. Shaposhnikov, A. Karavainikov, A. Prokopov, Y. M. Kharchenko, I. Lukienko, O. Miloslavskaya, and M. Kharchenko, Optimization of one-dimensional photonic crystals with double layer magneto-active defect, *Optical Materials* **78**, 521 (2018).
  - [22] G. Yu, H. Yang, J. Fu, X. Zhang, and R. Cao, Nonreciprocal transmission using a multilayer magneto-optical dispersive material with defect, *Journal of Electromagnetic Waves and Applications* **34**, 1400 (2020).
  - [23] A. A. Voronov, D. Karki, D. O. Ignatyeva, M. A. Kozhaev, M. Levy, and V. I. Belotelov, Magneto-optics of subwavelength all-dielectric gratings, *Optics Express* **28**, 17988 (2020).
  - [24] A. I. Chernov, M. A. Kozhaev, D. O. Ignatyeva, E. N. Beginin, A. V. Sadovnikov, A. A. Voronov, D. Karki, M. Levy, and V. I. Belotelov, All-dielectric nanophotonics enables tunable excitation of the exchange spin waves, *Nano letters* **20**, 5259 (2020).

- [25] F. Royer, B. Varghese, E. Gamet, S. Neveu, Y. Jourlin, and D. Jamon, Enhancement of both faraday and kerr effects with an all-dielectric grating based on a magneto-optical nanocomposite material, *ACS omega* **5**, 2886 (2020).
- [26] L. Bsawmaii, E. Gamet, F. Royer, S. Neveu, and D. Jamon, Longitudinal magneto-optical effect enhancement with high transmission through a 1d all-dielectric resonant guided mode grating, *Optics express* **28**, 8436 (2020).
- [27] V. Belotelov and A. Zvezdin, Magneto-optics and extraordinary transmission of the perforated metallic films magnetized in polar geometry, *Journal of Magnetism and Magnetic Materials* **300**, e260 (2006).
- [28] A. López-Ortega, M. Zapata-Herrera, N. Maccaferri, M. Pancaldi, M. Garcia, A. Chuvilin, and P. Vavassori, Enhanced magnetic modulation of light polarization exploiting hybridization with multipolar dark plasmons in magnetoplasmonic nanocavities, *Light: Science & Applications* **9**, 1 (2020).
- [29] A. N. Kalish, R. S. Komarov, M. A. Kozhaev, V. G. Achanta, S. A. Dagesyan, A. N. Shaposhnikov, A. R. Prokopov, V. N. Berzhansky, A. K. Zvezdin, and V. I. Belotelov, Magnetoplasmonic quasicrystals: an approach for multiband magneto-optical response, *Optica* **5**, 617 (2018).
- [30] N. Maccaferri, X. Inchausti, A. García-Martín, J. C. Cuevas, D. Tripathy, A. O. Adeyeye, and P. Vavassori, Resonant enhancement of magneto-optical activity induced by surface plasmon polariton modes coupling in 2d magnetoplasmonic crystals, *ACS Photonics* **2**, 1769 (2015).
- [31] G. Armelles, A. Cebollada, A. García-Martín, and M. U. González, Magnetoplasmonics: magnetoplasmonics: combining magnetic and plasmonic functionalities, *Advanced Optical Materials* **1**, 2 (2013).
- [32] K. Lodewijks, N. Maccaferri, T. Pakizeh, R. K. Dumas, I. Zubritskaya, J. Åkerman, P. Vavassori, and A. Dmitriev, Magnetoplasmonic design rules for active magneto-optics, *Nano letters* **14**, 7207 (2014).
- [33] A. E. Khramova, D. O. Ignatyeva, M. A. Kozhaev, S. A. Dagesyan, V. N. Berzhansky, A. N. Shaposhnikov, S. V. Tomilin, and V. I. Belotelov, Resonances of the magneto-optical intensity effect mediated by interaction of different modes in a hybrid magnetoplasmonic heterostructure with gold nanoparticles, *Optics express* **27**, 33170 (2019).
- [34] D. O. Ignatyeva, D. Karki, A. A. Voronov, M. A. Kozhaev, D. M. Krichevsky, A. I. Chernov, M. Levy, and V. I. Belotelov, All-dielectric magnetic metasurface for advanced light control in dual polarizations combined with high-q resonances, *Nature communications* **11**, 1 (2020).
- [35] J. Qin, L. Deng, T. Kang, L. Nie, H. Feng, H. Wang, R. Yang, X. Liang, T. Tang, J. Shen, *et al.*, Switching the optical chirality in magnetoplasmonic metasurfaces using applied magnetic fields, *ACS nano* **14**, 2808 (2020).
- [36] Y. Bi, L. Huang, X. Li, and Y. Wang, Magnetically controllable metasurface and its application, *Frontiers of Optoelectronics* , 1 (2021).
- [37] W. Yang, Q. Liu, H. Wang, Y. Chen, R. Yang, S. Xia, Y. Luo, L. Deng, J. Qin, H. Duan, *et al.*, Observation of optical gyromagnetic properties in a magneto-plasmonic metamaterial, *Nature communications* **13**, 1 (2022).
- [38] S. Xia, D. O. Ignatyeva, Q. Liu, H. Wang, W. Yang, J. Qin, Y. Chen, H. Duan, Y. Luo, O. Novák, *et al.*, Circular displacement current induced anomalous magneto-optical effects in high index mie resonators, *Laser & Photonics Reviews* **16**, 2200067 (2022).
- [39] R. Fujikawa, A. Baryshev, J. Kim, H. Uchida, and M. Inoue, Contribution of the surface plasmon resonance to optical and magneto-optical properties of a bi: Yig-au nanostructure, *Journal of Applied Physics* **103**, 07D301 (2008).
- [40] A. Baryshev, H. Uchida, and M. Inoue, Peculiarities of plasmon-modified magneto-optical response of gold-garnet structures, *JOSA B* **30**, 2371 (2013).
- [41] B. Fan, M. E. Nasir, L. H. Nicholls, A. V. Zayats, and V. A. Podolskiy, Magneto-optical metamaterials: Non-reciprocal transmission and faraday effect enhancement, *Advanced Optical Materials* **7**, 1801420 (2019).
- [42] S. Baek, A. V. Baryshev, and M. Inoue, Multiple bragg diffraction in magnetophotonic crystals, *Applied Physics Letters* **98**, 101111 (2011).
- [43] A. M. Grishin and S. Khartsev, Waveguiding in all-garnet heteroepitaxial magneto-optical photonic crystals, *JETP Letters* **109**, 83 (2019).
- [44] S. Tomilin, V. Berzhansky, A. Shaposhnikov, A. Prokopov, A. Karavaynikov, E. Milyukova, T. Mikhailova, and O. Tomilina, Vertical displacement of the magneto-optical hysteresis loop in the magnetoplasmonic nanocomposite, *Physics of the Solid State* **62**, 144 (2020).
- [45] M. Vasiliev, V. I. Belotelov, A. N. Kalish, V. A. Kotov, A. K. Zvezdin, and K. Alameh, Effect of oblique light incidence on magneto-optical properties of one-dimensional photonic crystals, *IEEE transactions on magnetics* **42**, 382 (2006).
- [46] D. Ignatyeva and V. Belotelov, Bound states in the continuum enable modulation of light intensity in the faraday configuration, *Optics Letters* **45**, 6422 (2020).
- [47] I. L. Lyubchanskii, N. N. Dadoenkova, M. I. Lyubchanskii, E. A. Shapovalov, A. E. Zabolotin, Y. P. Lee, and T. Rasing, Response of two-defect magnetic photonic crystals to oblique incidence of light: Effect of defect layer variation, *Journal of Applied Physics* **100**, 096110 (2006).
- [48] R. Schäfer, P. M. Oppeneer, A. V. Ognev, A. S. Samardak, and I. V. Soldatov, Analyzer-free, intensity-based, wide-field magneto-optical microscopy, *Applied Physics Reviews* **8** (2021).
- [49] G. Krinchik, E. Chepurova, and S. V. Ehgamov, Magneto-optical intensity effects in ferromagnetic metals and dielectrics.[bicavfe/sub 5/o/sub 12/], *Zh. Eksp. Teor. Fiz.:(USSR)* **74** (1978).
- [50] B.-R. Wu, J.-H. Yang, P. S. Pankin, C.-H. Huang, W. Lee, D. N. Maksimov, I. V. Timofeev, and K.-P. Chen, Quasi-bound states in the continuum with temperature-tunable q factors and critical coupling point at brewster's angle, *Laser & Photonics Reviews* **15**, 2000290 (2021).
- [51] N. Ansari, S. Khartsev, and A. Grishin, Multicolor filter all-garnet magneto-optical photonic crystals, *Optics letters* **37**, 3552 (2012).
- [52] N. C. Passler and A. Paarmann, Generalized 4× 4 matrix formalism for light propagation in anisotropic stratified media: study of surface phonon polaritons in polar dielectric heterostructures, *JOSA B* **34**, 2128 (2017).
- [53] L. Li, Fourier modal method for crossed anisotropic gratings with arbitrary permittivity and permeability ten-

- sors, Journal of Optics A: Pure and Applied Optics **5**, 345 (2003).
- [54] R. Danneau, P. Warin, J. Attané, I. Petej, C. Beigné, C. Fermon, O. Klein, A. Marty, F. Ott, Y. Samson, and M. Viret, Individual domain wall resistance in submicron ferromagnetic structures, Physical review letters **88**, 157201 (2002).
- [55] G. Dieterle, J. Förster, H. Stoll, A. Semisalova, S. Finizio, A. Gangwar, M. Weigand, M. Noske, M. Fähnle, I. Bykova, J. Grafe, D. Bozhko, H. Musiienko-Shmarova, V. Tiberkevich, A. Slavin, C. Back, J. Raabe, G. Schutz, and S. Wintz, Coherent excitation of heterosymmetric spin waves with ultrashort wavelengths, Physical review letters **122**, 117202 (2019).
- [56] V. Sluka, T. Schneider, R. A. Gallardo, A. Kákay, M. Weigand, T. Warnatz, R. Mattheis, A. Roldán-Molina, P. Landeros, V. Tiberkevich, *et al.*, Emission and propagation of 1d and 2d spin waves with nanoscale wavelengths in anisotropic spin textures, Nature nanotechnology **14**, 328 (2019).



# Supplementary Information

## Asymmetric Faraday Effect in a Magnetophotonic Crystal

D.O. Ignatyeva,<sup>1,2,3</sup> T.V. Mikhailova,<sup>1</sup> P.O. Kapralov,<sup>3</sup> S.D. Lyashko,<sup>1</sup> V.N. Berzhansky,<sup>1</sup> and V.I. Belotelov<sup>1,2,3</sup>

<sup>1</sup>*Institute of Physics and Technology, V.I. Vernadsky Crimean Federal University, 295007 Simferopol, Crimea*

<sup>2</sup>*Photonic and Quantum technologies school, Faculty of Physics,  
Lomonosov Moscow State University, Leninskie gori, 119991 Moscow, Russia*

<sup>3</sup>*Russian Quantum Center, 121205 Moscow, Russia*

(Dated: September 12, 2023)

### CONTENTS

S1. Magneto-optical tensor and effects	1
S1.1. Permittivity tensor and normal-mode equation for the magneto-optical media	1
S1.2. The Faraday rotation: odd magneto-optical effect	1
S1.3. Magnetic linear birefringence: even magneto-optical effect	2
S2. Material parameters and simulations	2
S2.1. Numerical simulations via transfer matrix method	2
S2.2. Material parameters	2
S3. Experimental measurements	3
S3.1. Magneto-optical hysteresis loops	3
S3.2. MPC optical and magneto-optical spectra	3
S3.3. Faraday rotation measurements via balanced scheme	3
S4. Symmetry break as the origin of the asymmetric Faraday effect	4
References	5

### S1. MAGNETO-OPTICAL TENSOR AND EFFECTS

#### S1.1. Permittivity tensor and normal-mode equation for the magneto-optical media

Magneto-optical properties of the isotropic magnetic material could be described by the following constitutive equations [1]:

$$\mathbf{D} = \varepsilon_0 \mathbf{E} + i[\mathbf{g} \times \mathbf{E}] + b(\mathbf{E} - \mathbf{m}(\mathbf{m} \cdot \mathbf{E})), \quad (1)$$

where  $\varepsilon_0$  is a permittivity of a non-magnetized medium,  $\mathbf{m} = \mathbf{M}/M$  is a unitary vector co-directed with medium magnetization,  $M = |\mathbf{M}|$  is magnetization absolute value,  $\mathbf{g} = \alpha \mathbf{M}$  is a gyration vector,  $b(M) = \beta \mathbf{M}^2 = \varepsilon_M - \varepsilon_0$  is the quadratic in magnetization coefficient. This corresponds to the Hermitian type of the permittivity tensor  $\varepsilon_{ij} = \varepsilon_{ji}^*$ , which for the magnetization along

the z-axis has the form:

$$\hat{\varepsilon} = \begin{pmatrix} \varepsilon_M & ig & 0 \\ -ig & \varepsilon_M & 0 \\ 0 & 0 & \varepsilon_0 \end{pmatrix}. \quad (2)$$

According to the Onsager principle, antisymmetric  $\mathbf{g}$  and symmetric  $b(M)$  magneto-optical contributions to the permittivity tensor are odd and even with respect to time reversal, and, consequently, linear and quadratic in medium magnetization [2].

Depending on the mutual orientation of light  $\mathbf{E}$ ,  $\mathbf{k}$  vectors and medium magnetization  $\mathbf{M}$ , both odd and even in magnetization effects could be observed. These effects are described by the normal-mode equation, which is directly derived from Maxwell's equations:

$$n^2 \mathbf{E} - \mathbf{n}(\mathbf{n} \cdot \mathbf{E}) = \mathbf{D}, \quad (3)$$

where  $\mathbf{n} = \mathbf{k}/k_0$  is the refractive index vector.

#### S1.2. The Faraday rotation: odd magneto-optical effect

The Faraday magneto-optical effect arises when the light travels along the magnetization direction,  $\mathbf{m} \parallel \mathbf{k}$ . The normal mode equation (3) has a solution in the form of the two circularly polarized modes,  $\sigma^+$  and  $\sigma^-$ , with the different refractive indices:

$$n_{\pm}^2 = \varepsilon_M \left( 1 \pm \frac{g}{\varepsilon_M} \right). \quad (4)$$

The difference between the refractive indices of  $\sigma^+$  and  $\sigma^-$  causes the rotation of the linearly polarized light propagating a distance  $L$  in such a medium:

$$\begin{aligned} \Phi &= -\frac{1}{2} k_0 L (n_+ - n_-) = \\ &= -\frac{1}{2} k_0 L \sqrt{\varepsilon_M} \left( \sqrt{1 + \frac{g}{\varepsilon_M}} - \sqrt{1 - \frac{g}{\varepsilon_M}} \right). \end{aligned} \quad (5)$$

The gyration coefficient  $g$  is usually much smaller than permittivity; for example, it is about  $g \sim 0.01 \dots 0.001$  for iron-garnets of different compositions [1] while the typical permittivity is in the range  $\varepsilon_0 = 4.5 \dots 6.5$ . For the considered iron-garnet at  $\lambda = 715$  nm wavelength



$\varepsilon_0 = 6.858 + 0.014i$ , and  $g = 0.021$  (see Sec. S2S2.2). Thus, one can make the Taylor-series expansion:

$$\begin{aligned}
\Phi &= \\
& -\frac{1}{2}k_0L\left(\sqrt{\varepsilon_0} + \frac{b}{2\sqrt{\varepsilon_0}}\right)\left(1 + \frac{1}{2}\frac{g}{\varepsilon_M} - \frac{1}{8}\frac{g^2}{\varepsilon_M^2} + \frac{1}{16}\frac{g^3}{\varepsilon_M^3} - \dots\right. \\
& \quad \left. - 1 + \frac{1}{2}\frac{g}{\varepsilon_M} + \frac{1}{8}\frac{g^2}{\varepsilon_M^2} + \frac{1}{16}\frac{g^3}{\varepsilon_M^3} + \dots\right) = \\
& = -\frac{1}{2}k_0L\left(\sqrt{\varepsilon_0} + \frac{b}{2\sqrt{\varepsilon_0}}\right)\left(\frac{g}{\varepsilon_M} + \frac{1}{8}\frac{g^3}{\varepsilon_M^3} + \dots\right) = \\
& = -\frac{1}{2}k_0L\left(\sqrt{\varepsilon_0} + \frac{b}{2\sqrt{\varepsilon_0}}\right)\left(\frac{g}{\varepsilon_0} - \frac{gb}{\varepsilon_0^2} + \frac{1}{8}\frac{g^3}{\varepsilon_0^3} + \dots\right) = \\
& = -\frac{1}{2}k_0L\frac{g}{\sqrt{\varepsilon_0}}\left(1 - \frac{b}{2\varepsilon_0} + \frac{1}{8}\frac{g^2}{\varepsilon_0^2} + \dots\right) = \\
& = -\frac{1}{2}k_0L\frac{\alpha}{\sqrt{\varepsilon_0}}\left(M - \frac{\beta M^3}{2\varepsilon_0} + \frac{1}{8}\frac{\alpha^2 M^3}{\varepsilon_0^2}\right). \tag{6}
\end{aligned}$$

The obtained formula illustrates the well-known property of the Faraday effect, which is odd in magnetization direction. Even when higher orders of  $M$  expansion terms are considered, it is clear that  $\Phi$  does not contain any even in magnetization terms. The next non-zero term in  $\Phi$  is proportional to  $M^3$  and is  $(-\beta/2\varepsilon_0 + \alpha^2/8\varepsilon_0^2) \sim 10^{-6}$  times smaller than the first linear one and definitely can be neglected. The oddness of the Faraday effect in the magnetization is a consequence of the time-reversal symmetry. The time reversal simultaneously changes the magnetization direction  $\mathbf{m} \rightarrow -\mathbf{m}$  and the light helicity  $\sigma^+ \rightarrow \sigma^-$ .

### S1.3. Magnetic linear birefringence: even magneto-optical effect

The magnetic linear birefringence arises if the medium is magnetized perpendicular to the light propagation direction:  $\mathbf{m} \perp \mathbf{k}$ . In this case, normal mode equation (3) has the solution in the form of the two linearly polarized waves,  $\mathbf{E} \parallel \mathbf{m}$  and  $\mathbf{E} \perp \mathbf{m}$  with different refractive indices:

$$n_{\parallel}^2 = \varepsilon_0, \tag{7}$$

$$n_{\perp}^2 = \varepsilon_M - \frac{g^2}{\varepsilon_0}. \tag{8}$$

The difference between the refractive indices of these two linearly polarized waves is:

$$n_{\perp} - n_{\parallel} = \frac{1}{2\sqrt{\varepsilon_0}}\left(b - \frac{g^2}{\varepsilon_0}\right) = \frac{1}{2\sqrt{\varepsilon_0}}\left(\beta - \frac{\alpha^2}{\varepsilon_0}\right)M^2 \tag{9}$$

Notice that  $n_{\perp} - n_{\parallel}$  contains only even in magnetization terms. This can be understood on the basis of time reversal which results in  $\mathbf{m} \rightarrow -\mathbf{m}$ , but both of these directions are equivalent from the point of view of linearly

polarized light with  $\mathbf{k} \perp \mathbf{m}$ . Namely, this configuration corresponds to the orientational magneto-optical effect which arises from the Fresnel coefficients difference for  $\mathbf{E} \parallel \mathbf{m}$  and  $\mathbf{E} \perp \mathbf{m}$  polarizations, and Coutton-Mouton effect which reveals itself in appearance of the magneto-optical ellipticity similar to the case of the natural birefringence. It can be clearly seen that both effects related to such configuration are  $\sim 10^{-3}$  times smaller than the ones observed for a Faraday configuration.

An important consequence of Eq. (7), (8) is that the magnetization of the sample perpendicular to the light plane of incidence (which is also called the transverse configuration) does not produce the magneto-optical polarization rotation of light. Thus, this configuration is used to determine the purely optical contribution to the rotation of the mixed polarization state which arises due to the Fresnel reflection at the interfaces of the magnetophotonic crystal layers.

## S2. MATERIAL PARAMETERS AND SIMULATIONS

### S2.1. Numerical simulations via transfer matrix method

Numerical simulations of the optical and magneto-optical spectra of the magnetophotonic crystal were performed by numerical solution of Maxwell's equations by the transfer matrix method  $4 \times 4$ . The details on this method are provided in [3]. Each of the layers of the magnetophotonic crystal was described by the permittivity tensor, so that  $\varepsilon_{ij} = i\epsilon_{ijk}g_k$  [1], where  $\epsilon_{ijk}$  is a Levi-Civita symbol and  $g_k$  are the components of the gyration vector that is parallel to the magnetization of the material. Actually,  $g_k$  was non-zero only for ferrimagnetic  $\text{Bi}_{2.97}\text{Er}_{0.03}\text{Al}_{0.5}\text{Ga}_{0.5}\text{O}_{12}$  (BIG) garnet.

The wavelength dependence of all of the permittivity tensor components was taken into account, as well as the Fresnel reflection from the backside of a transparent substrate. The exact values of these components provided in Sec. S2S2.2.

The transfer matrix method provides the optical characteristics of the structure, such as transmittance, reflectance, absorption, polarization rotation, and others.

### S2.2. Material parameters

The following wavelength-dependent material parameters were used for the simulations. The refractive index of (111)  $\text{Gd}_3\text{Ga}_5\text{O}_{12}$  (GGG) substrate is equal to

$$n_{\text{GGG}} = 1.91 + \left(\frac{203[\text{nm}]}{\lambda}\right)^2, \tag{10}$$

and the refractive index of air is  $n_{\text{air}} = 1$ .

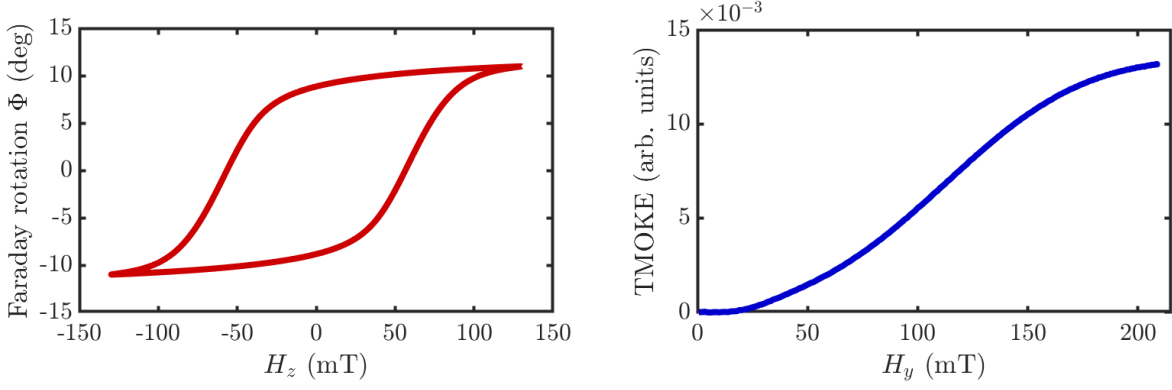


FIG. S2.1: Experimental hysteresis loops obtained for the magnetophotonic crystal.

The refractive index of diamagnetic  $\text{Sm}_3\text{Ga}_5\text{O}_{12}$  (SGG) material  $n_{\text{SGG}} = \sqrt{\epsilon_{\text{SGG}}}$  has the form:

$$\epsilon_{\text{SGG}} = 1 + \frac{2.75}{1 - \left(\frac{128[\text{nm}]}{\lambda}\right)^2}; \quad (11)$$

The refractive index of the magneto-optical ferrimagnetic  $\text{Bi}_{2.97}\text{Er}_{0.03}\text{Al}_{0.5}\text{Ga}_{0.5}\text{O}_{12}$  (BIG) garnet is:

$$n_{\text{BIG}} = 1 + \frac{4.70}{1 - \left(\frac{303[\text{nm}]}{\lambda}\right)^2} + \frac{0.08}{1 - \left(\frac{494[\text{nm}]}{\lambda}\right)^2} + i \cdot 0.07 \cdot \frac{494[\text{nm}]}{\lambda}, \quad (12)$$

while its magneto-optical activity is described by the gyration coefficient:

$$g = 0.40 - 1.85 \cdot 10^{-3}[\text{nm}^{-1}]\lambda + 3.23 \cdot 10^{-6}[\text{nm}^{-2}]\lambda^2 - 2.49 \cdot 10^{-9}[\text{nm}^{-3}]\lambda^3 + 7.22 \cdot 10^{-13}[\text{nm}^{-4}]\lambda^4. \quad (13)$$

These values were determined from the optical and magneto-optical spectra of the samples and agree with the ones reported for the garnets with similar compositions [4, 5].

### S3. EXPERIMENTAL MEASUREMENTS

#### S3.1. Magneto-optical hysteresis loops

All measurements were performed at room temperature. First, the magneto-optical hysteresis loops of the Faraday effect at normal incidence were measured (Fig. S2.1a). The out-of-plane coercive magnetic field needed to saturate the sample is  $H_{zc} = 120$  mT. This agrees well with the previous results obtained for similar materials [4].

Sample characterization for the in-plane configuration of the applied external magnetic fields was performed using the transverse magneto-optical Kerr effect (TMOKE)

measurements for the oblique incidence of p-polarized light (Fig. S2.1b). The TMOKE value was measured as the reflected light intensity change for the magnetic field changing from  $+H_y$  to  $-H_y$ , so that  $\text{TMOKE} = I(+H_y) - I(-H_y)$ . The in-plane coercive magnetic field needed to saturate the sample is  $H_{yc} = 200$  mT.

In our further experiments, we used the magnetic fields exceeding these values,  $H_z = 220$  mT and  $H_y = 370$  mT, correspondingly, in order to ensure that magnetization was aligned with the external magnetic field.

#### S3.2. MPC optical and magneto-optical spectra

Figure S3.2 shows the transmittance and Faraday rotation spectra for p- and s-polarized light at different angles of incidence. It is clearly seen that the difference between the two polarization increases with the increase of the angle of incidence. This can be explained by the growing difference between the Fresnel reflection coefficients and consequent difference of the reflectance of the Bragg mirrors surrounding the cavity layer of the MPC. This results in the increase of the Q-factor difference of the p-polarized and s-polarized cavity mode, resulting in the several times different transmittance and Faraday rotation observed for these polarizations (Fig. S3.2).

Thus, at the oblique incidence the system is sensitive to the mutual orientation of  $\mathbf{k}_r$  and  $\mathbf{E}$ . The more pronounced this difference is, the higher inequality of counter- and clockwise rotations of the intermediate polarisation could be expected. Thus, AFE is expected to increase with the increase of the angle of incidence.

#### S3.3. Faraday rotation measurements via balanced scheme

To measure the Faraday rotation  $\Phi(M_z)$  one might determine the magneto-optical contribution to the total polarization rotation acquired by the light during the propagation in a magnetic structure. In the most general case, the total polarization rotation TR has both purely

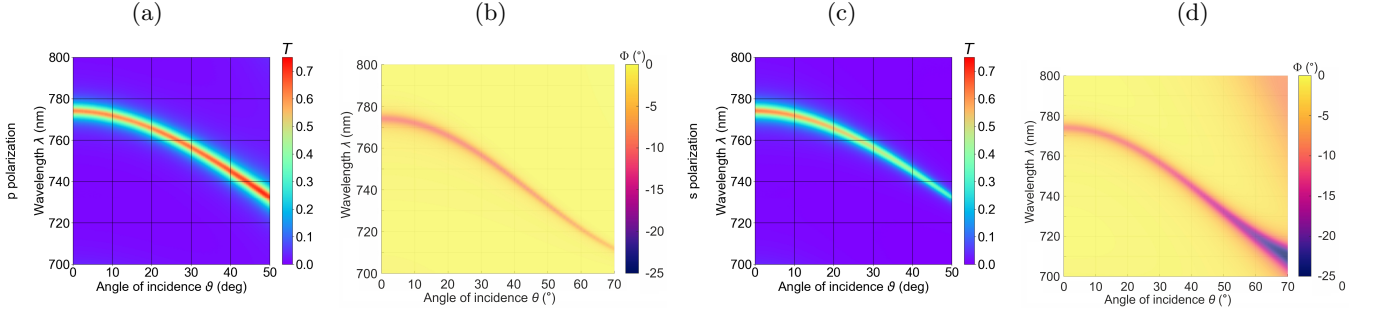


FIG. S3.2: Wavelength vs. incidence angle spectra of (a),(c) experimentally measured transmittance and (b),(d) simulated Faraday rotation  $\Phi(+M_z)$  for p- (left pane) and s-polarized (right pane) light.

optical and magneto-optical contributions:

$$TR = OR + \Phi(M_z). \quad (14)$$

Purely optical polarization rotation might exist in the structure, for example, due to the Fresnel reflection or other magnetization-independent effects. Thus, this contribution should be taken into account and eliminated in the measurements.

As the Faraday rotation  $\Phi$  is usually odd in the magnetization (see Eq. (6)), its contribution can be determined in one of the two equivalent ways, as  $\Phi(M_z) = \frac{1}{2}(TR(+M_z) - TR(-M_z))$  or  $\Phi(M_z) = (TR(+M_z) - TR(M_z = 0))$ . For the case where the asymmetric Faraday rotation is expected, one might use the later formula and measure TR for  $+M_z$ ,  $-M_z$  and  $M_z = 0$  separately.

The measurements of the total polarization rotation  $TR$  can be performed in different ways. One of the well-known methods providing high precision is based on a so-called balanced scheme with additional polarizer. If a polarizer is installed after the magnetic structure and aligned at an angle  $\alpha$  with respect to the polarization of the incident linearly polarized light, then the intensity of light transmitted through this polarizer equals to

$$I_{\text{out}} = I_0 \cos^2(\alpha + TR). \quad (15)$$

In the balanced scheme, the polarizer is aligned at  $\alpha = \pi/4$  angle with respect to the incident polarization of light. Therefore, according to Eq. (15) the intensity of light transmitted through the polarizer equals to

$$\begin{aligned} I_{\text{out}} &= I_0 \cos^2\left(\frac{\pi}{4} + TR\right) = \\ &= \frac{I_0}{2} \left( \cos\left(2\left(\frac{\pi}{4} + TR\right)\right) + 1 \right) = \\ &= \frac{I_0}{2} (1 - \sin(2TR)) \end{aligned} \quad (16)$$

In order to make it possible to reveal the difference between the values of  $\Phi(+M_z)$  and  $\Phi(-M_z)$ , the following measurements were performed:

1. The transmittance  $I_0(\lambda)$  of the MPC without additional polarized was measured.

## 2. The purely optical rotation

$$OR(\lambda) = \frac{1}{2} \text{asin} \left( 1 - \frac{2I_{M_z=0}^{\pi/4}(\lambda)}{I_0(\lambda)} \right) \quad (17)$$

was determined from the measurements of the transmitted intensity  $I_{M_z=0}^{\pi/4}(\lambda)$  in a balanced scheme with additional  $\pi/4$ -tilted polarizer and in-plane magnetic field applied to the structure to provide  $M_z = 0$  (see also Sec. S1 S1.3)

3. In accordance to Eq. (16), the Faraday rotation for  $+M_z$  and  $-M_z$  magnetizations was measured as

$$\Phi(\pm M_z) = \frac{1}{2} \text{asin} \left( 1 - \frac{2I_{\pm M_z}^{\pi/4}(\lambda)}{I_0(\lambda)} \right) - OR(\lambda). \quad (18)$$

The transmitted intensity  $I_{\pm M_z}^{\pi/4}(\lambda)$  was measured separately for  $+M_z$  and  $-M_z$  magnetization directions in a balanced scheme with additional  $\pi/4$ -tilted polarizer.

Thus, a step-by-step experimental measurements were performed to reveal AFE and to take into account possible changes of the transmitted light intensity and optical rotation due to the purely optical effects.

## S4. SYMMETRY BREAK AS THE ORIGIN OF THE ASYMMETRIC FARADAY EFFECT

Asymmetric Faraday effect (AFE) arises due to the symmetry break which can be described by an in-plane director oriented at the non-zero angle to  $\mathbf{E}$ . Such configuration is non-symmetric with respect to the reflection in the mirror placed parallel to  $\mathbf{M}$ . While the detailed analysis is provided in the main text, let us illustrate how this asymmetry causes the non-equivalence between the the clock- and counterclockwise directions of polarization rotation. Figure S4.4 schematically shows the configuration characterized by a director  $\mathbf{L}$  oriented along  $x$  axis. This causes the dependence of optical characteristic of a structure  $\Omega$  (which might be transmittance, absorption, etc.)

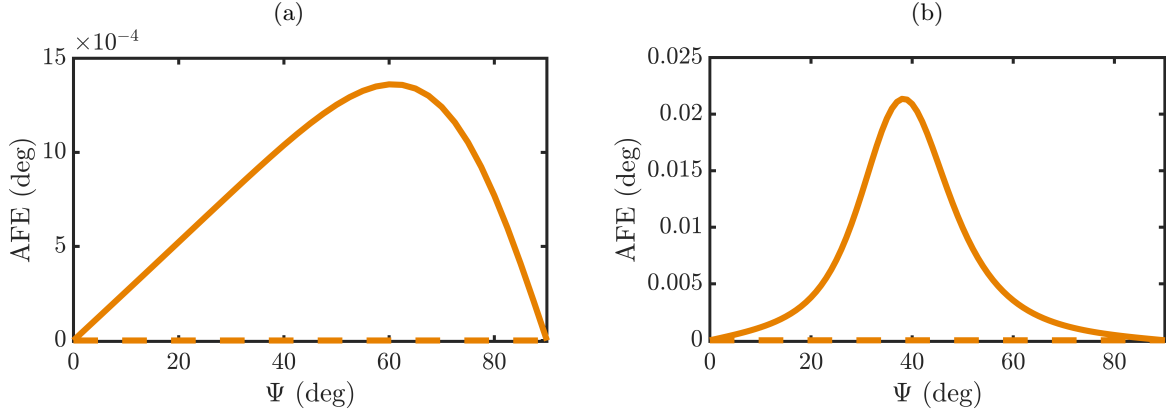


FIG. S3.3: Asymmetric Faraday effect caused by the spatial symmetry break. (a) Symmetry break by light: AFE arising for the oblique (solid line) and normal (dashed line) incidence on a smooth iron-garnet film on a  $\text{SiO}_2$  substrate. (b) Symmetry break caused by the structure: AFE arising at normal incidence in a smooth iron-garnet film covered by 1D Si grating (solid line) or smooth Si layer (dashed line).

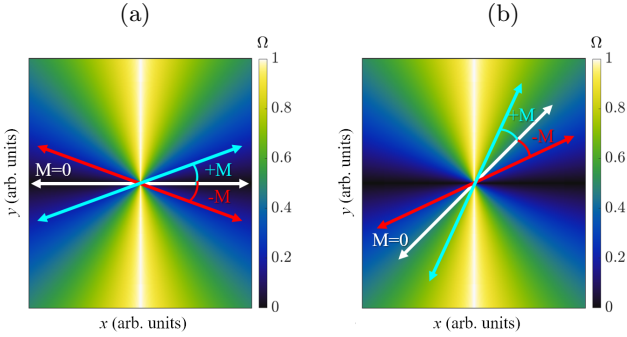


FIG. S4.4: Asymmetric Faraday effect arising as the result of non-equivalence of the counter- and clockwise rotation directions caused by the presence of the director  $L$  along  $x$ -axis and consequent polarization dependence of some optical characteristic  $\Omega$ . (a) Case of  $\mathbf{E}$  parallel to  $L$  and equivalence of clock and counter-clockwise rotations. (b) Case of  $\mathbf{E}$  tilted with respect to  $L$  which cause non-equivalence of clock and counter-clockwise rotations.

on the polarization direction, as shown by the pseudo-color plot in Fig. S4.4. It is clearly seen that if polarization of the light (white arrow) is parallel to  $L$  (Fig. S4.4a) than the rotations in clock- and counterclockwise directions are equivalent to each other, so  $+M$  and  $-M$  magnetisations induce the same magnitude of the Faraday polarization rotation (blue and red arrows, correspondingly). In contrast to this, if polarization of the light is tilted with respect to  $L$  (Fig. S4.4b) than the rotations in clock- and counterclockwise directions are not equivalent to each other. This might be seen in Fig. S4.4b, as

blue and red arrows denoting polarization  $\mathbf{E}$  correspond to different  $\Omega$  values. Thus, non-equivalence of counter- and clockwise rotations arise in this case.

Such symmetry breaking due to the presence of a director characterizing the light and structure configuration is a quite general condition. This means, that AFE might arise in various cases if the symmetry break is produced either by the light itself, or by the structure. Here we justify this statement by the numerical simulations of the two configurations.

Figure S3.3a demonstrates the AFE arising due to the symmetry break introduced by the light oblique incidence with  $\mathbf{k}_r$  vector on a smooth iron-garnet film. This situation is similar to the MPC discussed in the main text and also causes the appearance of AFE. AFE disappears for pure p- and s-polarized light ( $\Psi = 0$  and  $\Psi = 90$  deg points of a solid line in Fig. S3.3a) and at the normal incidence when  $\mathbf{k}_r = 0$  (dashed line in Fig. S3.3a).

On the contrary, Fig. S3.3b demonstrates the AFE arising due to the symmetry break introduced by the structure. Here, 1D Si grating is deposited on top of the smooth iron-garnet film. This configuration can be described by a director  $L$  oriented in a grating periodicity direction. Thus, even for a normal incidence if polarization is tilted with respect to  $L$ , i.e. in the case of polarisations intermediate between the ones parallel and perpendicular to the Si grating stripes, AFE is observed (solid line in Fig. S3.3b). AFE vanishes in the cases of  $\mathbf{E}$  parallel and perpendicular to the grating stripes ( $\Psi = 0$  and  $\Psi = 90$  deg points of a solid line in Fig. S3.3b), or if Si grating is transformed into the continuous Si layer and therefore preferred direction described by  $L$  disappears (dashed line in Fig. S3.3b).

[1] A. K. Zvezdin and V. A. Kotov, *Modern magnetooptics and magneto-optical materials* (CRC Press, 1997).

[2] A. M. Kalashnikova, A. V. Kimel, and R. V. Pisarev, *Ul-*

- trafast opto-magnetism, *Physics-Uspekhi* **58**, 969 (2015).
- [3] Š. Višňovský, M. Nývlt, V. Prosser, R. Lopusník, R. Urban, J. Ferré, G. Pénissard, D. Renard, and R. Krishnan, Polar magneto-optics in simple ultrathin-magnetic-film structures, *Physical Review B* **52**, 1090 (1995).
  - [4] A. M. Grishin and S. I. Khartsev, Luminescent magneto-optical photonic crystals, in *Journal of Physics: Conference Series*, Vol. 352 (IOP Publishing, 2012) p. 012007.
  - [5] A. M. Grishin and S. Khartsev, Waveguiding in all-garnet heteroepitaxial magneto-optical photonic crystals, *JETP Letters* **109**, 83 (2019).